ISSN 1225-827X (Print)
ISSN 2287-4623 (Online)
J Kor Soc Fish Technol, 50 (4), 435－446, 2014
http://dx.doi.org/10.3796/KSFT.2014.50.4.435

FISHERIES TECHNOLOGY
www.fishtech.or.kr
〈Original Article〉

Characteristics of tidal turbulence near the bottom at a coastal trench in Tongyoung, Korea

Yonghae KIM*, Chul-Hoon HONG[1]

Institute of Marine Industry, College of Marine Science, Gyeongsang National University, Tongyeong, 650-160, Republic of Korea

[1]Div. of Marine Production System Management, Pukyong National University, Busan, 608-737, Republic of Korea

Tidal turbulence was examined using three-dimensional tidal velocity data observed at a trench offshore of Tongyoung, Korea. The kinetic energy and intensity, including the variation period of the flow velocity and direction, were used to investigate the relationships between tidal turbulence and fishing gear dynamics, including the effects of swimming fish during fishing operations. As the resultant velocity increased from 0.2 to 0.9 m/s, the kinetic energy also significantly increased, while the turbulence intensity decreased from 50 to 10%. Tidal flow in strong flow fields displayed shorter periods of between 4 and 10 s, as determined by fast Fourier transform, the global wavelet method, and peak event analysis, and the periods were compared with the period of response to swimming fish and to oscillation of fishing gear. As mean velocity increased, velocity amplitude also increased from 0.1 to 0.6 m/s, and its directional amplitude changed markedly from 20 and 90°. Our study suggests that tidal turbulence can influence fish behavior or fishing gear geometry during fishing operations, although our analysis considered only a limited area. In future work, observations should be carried out over a more extensive depth and area.

Keywords: Tidal flow, Kinetic energy, Turbulence intensity, Period and amplitude

Introduction

Turbulence in tidal currents affects on the movement of animals and fishing gear operations. Recently, the turbulence flow as a three-dimensional (3-D) component of velocity was measured in coastal tides and analyzed using acoustic Doppler current profilers (ADCP) or acoustic Doppler velocimeters (ADV) (Thorpe, 2007).

The turbulence flow, which can be defined by the velocity field, is not repeatable in either the whole or part of the flow domain referred to as laminar flow (Bernard and Wallace, 2002). In nature, water is generally in a state of non-uniform and variable motion that is referred to as “turbulence”, although there exists no straightforward, unambiguous definition of the term (Thrope, 2007). Turbulence is generally accepted to be an energetic, rotational and eddying state of motion that results in the dispersion of material and the transfer of momentum, heat and solutes at rates far higher than those of molecular processes alone.

Turbulence is often dominated by coherent structure activities and turbulent events which may be defined as a series of turbulent fluctuations that contain more kinetic energy than the average turbulent fluctuations within the relevant section. Therefore, studies in tidal areas of 3-D turbulence structures have been hampered by the limited size of the observed area

*Corresponding author: yonghae@gnu.kr, Tel: 82-55-772-9183, Fax: 82-55-772-9189

due to equipment limitations; e.g., Laser Doppler Velocimetry in tank experiments (Pichot et al., 2009).

The characteristics of turbulence in tidal flow have been investigated in various contexts, such as sediment suspension (Ham et al., 2001; Chanson, 2010; Chanson et al., 2011; Yuan et al., 2009), tidal straining (Simpson et al., 2005; Thorpe et al., 2008), and tidal energy turbines (Rippeth et al., 2003; Thomson et al., 2012).

Turbulent flow can affect swimming fish (Shadwick and Lauder, 2006; Liao, 2007; Webb and Cotel, 2010; Tritico and Cotel, 2010) and fish escape from codends (Kim, 2012; 2013a). Flow inside codends was analyzed by measuring the turbulence intensity and periodicity for shrimp beam trawls and bottom trawls (Kim, 2012; 2013a). Flow inside codend towed fishing gear may be affected primarily by tidal flow, followed by wakes inside fishing gear (Bouhoubeiny et al., 2011) and ship motion including the wave effect (O'Neill et al., 2003). Turbulence measurements close to Korea were carried out in the western Yellow Sea off the coast of China in both relatively shallow (Liu et al., 2009a; 2009b; Yuan et al., 2009) and deeper (Lozovastsky et al., 2012) waters.

Thus, the 3-D components of tidal turbulence can affect animal kinetics such as swimming performance, or the drag or wake of fishing gear. However, tidal turbulence at the sea bottom has, to our knowledge, not been analyzed in Korean waters as precise high-frequency 3-D flow. Hence, the purpose of this preliminary study was to determine the physical elements of tidal turbulence, such as turbulence intensity and dominant period focused on fish movement and fishing gear dynamics. Two locations at a trench between Manjido and Bujido offshore of Tongyoung, Korea were selected for their different geological conditions and as locations used as the fishing grounds for shrimp beam trawls, two-boat seine nets, etc. 3-D flow measurement data were collected using ADV and the kinetic energy, turbulence intensity, and period in relation to fishing gear dynamics and movements of swimming fish during fishing operations were analyzed.

Materials and methods

Tidal flow was measured using a three-component acoustic Doppler velocimeter (Vector, Nortek, Norway) as described in previous studies (Kim, 2012; 2013a). The velocimeter was set in an upright position using a circular frame of 10-mm iron rods and 20-kg lead weights to anchor it firmly on the seabed (Fig. 1). The velocimeter measured water velocity based on a volume of water of 1.5-cm diameter 16 cm from the acoustic probe with an accuracy of ±0.5% according to the manufacturer's specifications. The overall length of the velocimeter was 82.5 cm; its diameter was 7.5 cm; and its weight in water was 1.5 kg. The instrument also included sensors for measuring temperature (accuracy, 0.1°C), direction (compass accuracy, 2°), tilt (pitch and roll accuracy, 0.2°), and depth pressure (accuracy, 0.25%). A holding frame that formed a quadratic pyramid (diameter 82 cm, height 63 cm) was used to maintain the device in the orthogonal position, maintaining its sampling position at 1 m above the seabed. The equipment was deployed with 8-mm PP rope of 1.5 times length of depth in connection with a 2.5 kg weight and a spherical buoy (diameter, 30 cm) to a upright rod with a flag on the surface.

Observations were performed at two sites at a deep trench between Manjido and Bujido south-west of Tongyoung, as shown in Fig. 2. The trench was oriented north-west to south-east at depths ranging between 50 and 70 m, while the depth of the surrounding area ranged between 30 and 40 m. These sites are generally used as the primary fishing ground

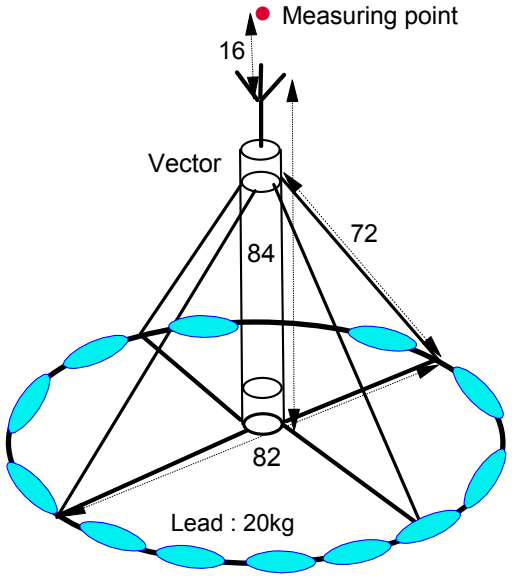

Fig. 1. Vector velocimeter set-up in the upright position with a circular frame (P: measuring position, units are cm).

of coastal fishing boats, including those using shrimp beam trawls and two-boat seine nets. Measurements were carried out five times (at sites S1, 2, 4, 5, 6) west of Manjido and once (site S3) north of Bujido. The sampling times and tidal conditions are shown in Table 1.

Tidal flow velocity was defined as three components: east (positive)-west (negative) velocity (V_x), north (positive)-south (negative) velocity (V_y), automatically designated by internal compass, and depth (V_z) directions. Vector measurements of tidal current were set at 2 m/s maximum velocity as a 3-D axis with east, north and depth directions with a 16-Hz sampling rate mostly at 34 practical salinity units (psu). The acoustic speed was also calibrated automatically using data from the temperature and pressure sensors, and all sampling data were stored in internal memory.

Following data collection at sea, the landing state of the data was checked using the tilt, noise and correlation data. When the standard deviation of the pitch or roll data per second was higher than the tilt accuracy; i.e., 0.2°, the vector could be shaking due to slack landing. Therefore, measurements taken at Stations S4 and S5 with a tilt of pitch and roll >1° were not included in the analysis (Parra et al., 2014). Additionally, for the 3-D flow velocity data, average signal to noise ratios <15dB and average correlation values <70% were eliminated (McLelland and Nicholas, 2000).

Based on the definition of turbulence flow in Bernard and Wallace (2002), the tidal turbulent flow was analyzed as turbulence intensity, kinetic energy and oscillation period for analysis of the fisheries variables. The three components (V_x, V_y, V_z) of velocity data for the entire measurement period for each site were assessed every 1 min (data n=480 = 8 Hz × 60 s or 960 = 16 Hz × 60 s) to determine turbulence intensity and kinetic energy, as shown in Table 2. The mean resultant velocity U_m represents an estimate for consecutive 1-min samples as follows:

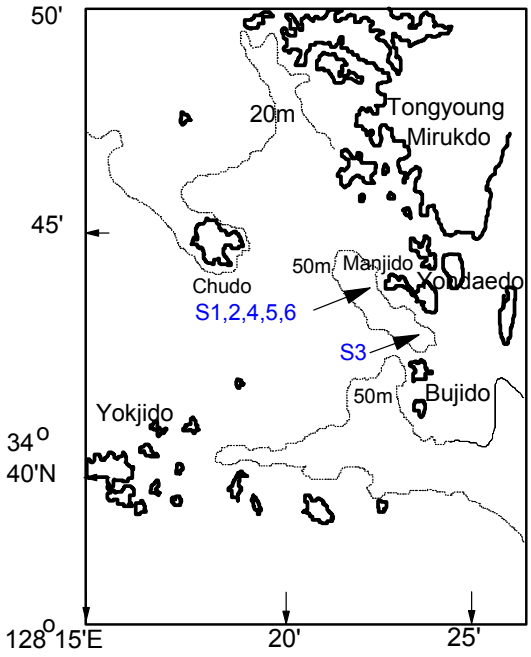

Fig. 2. Map of observation sites (S1–6) at a trench offshore of Tongyoung, Korea.

Table 1. Sampling stations and tidal conditions

Station	Lat. Long.	Depth (m)	Duration (start-end) (KST)	Sampling rate (Hz)	Tide day	Time (range)* (KST, cm)
S1	34° 44.2′N 128° 22.2′E	65	9:15-13:00, 27 Oct 2011	8	8	8:57(293) 14:55(27)
S2	34° 44.3′N 128° 22.1′E	65	13:58, 6 Apr-	16	8	14:22(-9) 20:54(274)
			16:13, 7 Apr 2012		9	9:05(265) 15:00(-18)
S3	34° 42.9′N 128° 23.8′E	60	10:10-20:50, 3 Dec 2013	16	8	9:02(282) 15:02(35)
S4	34° 44.1′N 128° 22.2′E	65	10:00-14:30, 4 Nov 2013	16	9	9:12(280) 15:11(40)
S5	34° 44.1′N 128° 22.2′E	65	20:00, 16 Nov-	16	6	20:05(230)
			06:37 17 Nov 2013		7	2:03(36) 8:32(262)
S6	34° 44.1′N 128° 22.2′E	68	20:50, 30 Mar-	16	7	20:57(267)
			8:07, 31 Mar 2014		8	2:53(2) 8:55(260)

* High and low tide with tidal difference from tide table

Table 2. Sampling times of turbulence intensity measurements and periods of strong flow

Station	Total sampling		Strong tide selection				
	Duration (min)	No. of measurements	Symbol	Start time (KST)	Flow	Duration (min)	No. of measurement
S1	215	103,050	S1a	9:31	Ebb	53	25,600
S2	1,576	1,513,119	S2a	17:17	Flood	18	16,820
			S2b	5:15	Flood	27	25,800
			S2c	7:26	Flood	13	12,200
			S2d	0:57	Ebb	17	15,600
S3	638	612,480	S3a	12:52	Ebb	83	80,401
			S3b	18:15	Flood	47	45,000
S6	671	644,160	S6a	4:00	Flood	38	36,100

$$U_m = (V_x^2 + V_y^2 + V_z^2)^{0.5} \quad (1)$$

Accordingly S_x, S_y, and S_z represent the standard deviation of flow velocities per minutefor V_x, V_y, and V_z, respectively. Then, turbulence kinetic energy (K_e, m^2/s^2)can be represented as:

$$K_e = (S_x^2 + S_y^2 + S_z^2) / 2 \quad (2)$$

Next , the turbulence intensity (T_r, %) as a ratio can be defined as the square root of K_e divided by the mean flow velocity U_m as:

$$T_r = K_e^{0.5} / U_m \quad (3)$$

For periodic analysis, each sampling dataset recorded at 8 and 16 Hz was converted for each resultant velocity (Vr) and horizontal flow direction (Ab) using the $V_x$and V_y components for strong tides of six flood durations and two ebb durations during each measurement (Table 2). Using these converted data, the specific period was estimated by fast Fourier transform (FFT), global wavelet method, and Morlet wavelet method.

MATLAB (MathWorks) was used to analyze the periodicity of the tidal flow velocity and direction for shorter periods <30 s using FFT for selected strong flood or ebb data from each measurement. The Morlet wavelet method in MATLAB was well localized in both time and space for periodicity analysis, as applied in many studies (Yuan et al., 2009; Seena and Sung, 2011). The Morlet continuous wavelet method (CWT) was also viewed for 2000 burst sampling data for shorter periods <10s, which was more relevant for the analysis of swimming fish (Kim et al., 2008) or fishing gear movements (O'Neill et al, 2003; Kim, 2012; 2013a). In addition, the global and Morlet wavelet spectra for velocity and direction were calculated to determine the moderate dominant period <30 s using software from Torrence and Compo (1998) and Zhang *et al*. (2010).

The above methods, however, are unable to calculate the amplitude as the velocity or directional range of a period, and are also unsuitable for periodic data with a wide range. Therefore, the event analysis method, such as the difference between peak and valley values, was adapted using software designed by ourselves based on Narasimha et al. (2007) to analyze the depth change of the shaking codend (Kim, 2013b). When the depth increased until the peak and then decreased in consecutive time series data, the peak value was detected as a positive peak value, and the valley value was detected as a negative valley value. Fig. 3 shows the results using the event analysis method for Station S2b. The minimum time interval between peaks or valleys was limited to 1 s, taking into consideration the sampling rate and oscillation of fishing gear (O'Neill et al., 2003; Kim, 2013a). The initial threshold value (Vi, +:peak, -:valley) between neighboring peaks or neighboring valleys was categorized by the mean value ± 0.5 SD for data at 30-s intervals, respectively. Then, a peak event value (Vp+ for peak, Vp- for valley) can be selected as the highest value among Vi. The mean period was estimated from the average of the total intervals between peaks and between valleys, while the mean amplitude was estimated from the velocity or directional difference between peak events and valley events that occurred only consecutively as a pair.

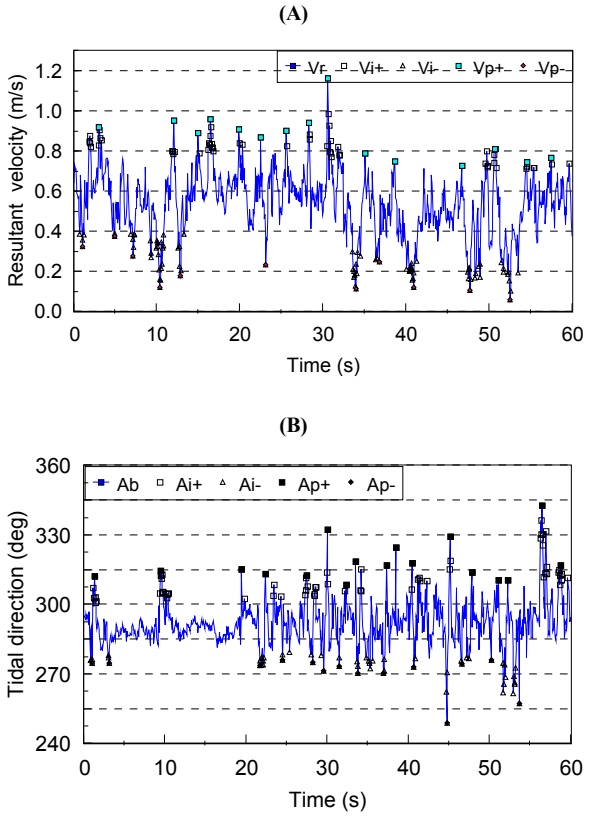

Fig. 3. Peak and valley events of the resultant velocity (A) and direction (B) from Station S2b.

V: velocity, A: tidal direction, Suffix r: resultant, i: initial threshold value, Suffix p: peak event, + :peak, -: valley)

Results and discussion

Fig. 4 shows the 3-D tidal velocities Vx west, Vy north, and Vz depth directions and their resultant velocity (Um) and tidal direction for data sampled at 16 Hz at flood tide at S2b given in Table 3. The 16-Hz sampling rate exhibited higher variations in flow velocity and flow direction as turbulence of tidal flow, although a higher sampling rate is needed to compare these variations.

Fig 5 shows the resultant mean tidal velocity for 1 min = 60 s resultant velocity (Fig. 4(B)) estimated from the 3-D data of east, north and depth velocity sampled at 16 Hz at Stations S2 and 6. Over the measurement period, the mean resultant velocity changed with tidal range while the flood velocity was greater than the ebb velocity.

The variation in velocity was represented as a kinetic energy as the absolute mean value >1 min using the resultant velocity yielded by Eq. (2), and as a turbulence intensity as the relative rate yielded by Eq. (3). The kinetic energy and turbulence intensity in relation to the mean resultant velocity at Station S3 are shown in Fig. 6. The kinetic energy E_k or turbulence intensity (T_r) can be expressed as a function of the resultant velocity by the following equations:

$$E_k = E_o U_m^a \quad (4)$$

$$T_r = T_o U_m^b \quad (5)$$

The turbulence intensity when the mean velocity was >0.2 m/s ranged between 10 and 50%, which was higher than the values of 8–15% recorded 4.7 m above the seabed at 22-m water depth in Puget Sound, USA and 10% recorded at a site off Seattle, USA (Thomson et al., 2012). The turbulence intensity affected the swimming speed of perch in tank experiments (Lupandin, 2005), and was the key variable affecting fish swimming in turbulent flow (Liao, 2007).

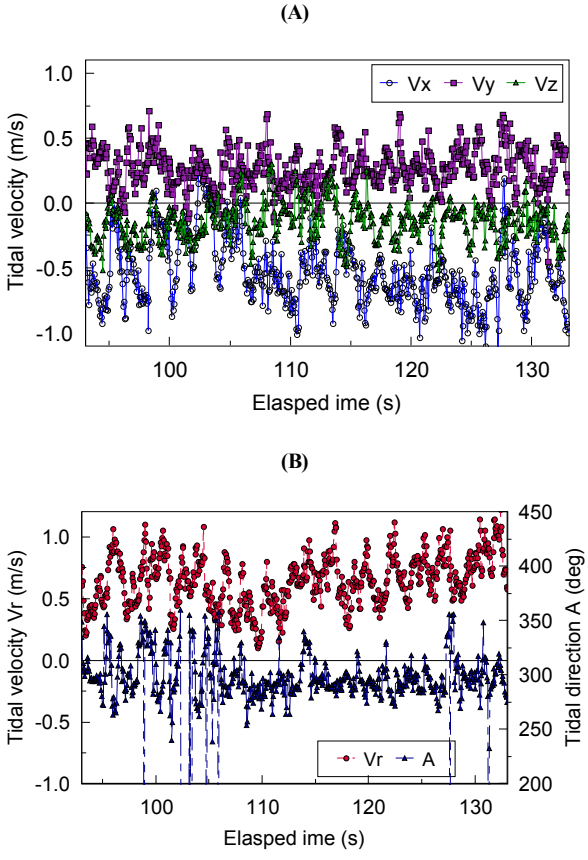

Fig. 4. 3-D tidal velocity, Vx east, Vy north, and Vz depth directions (A) and their resultant velocity and tidal direction (B) for the 16-Hz samples at S2b shown in Table 3.

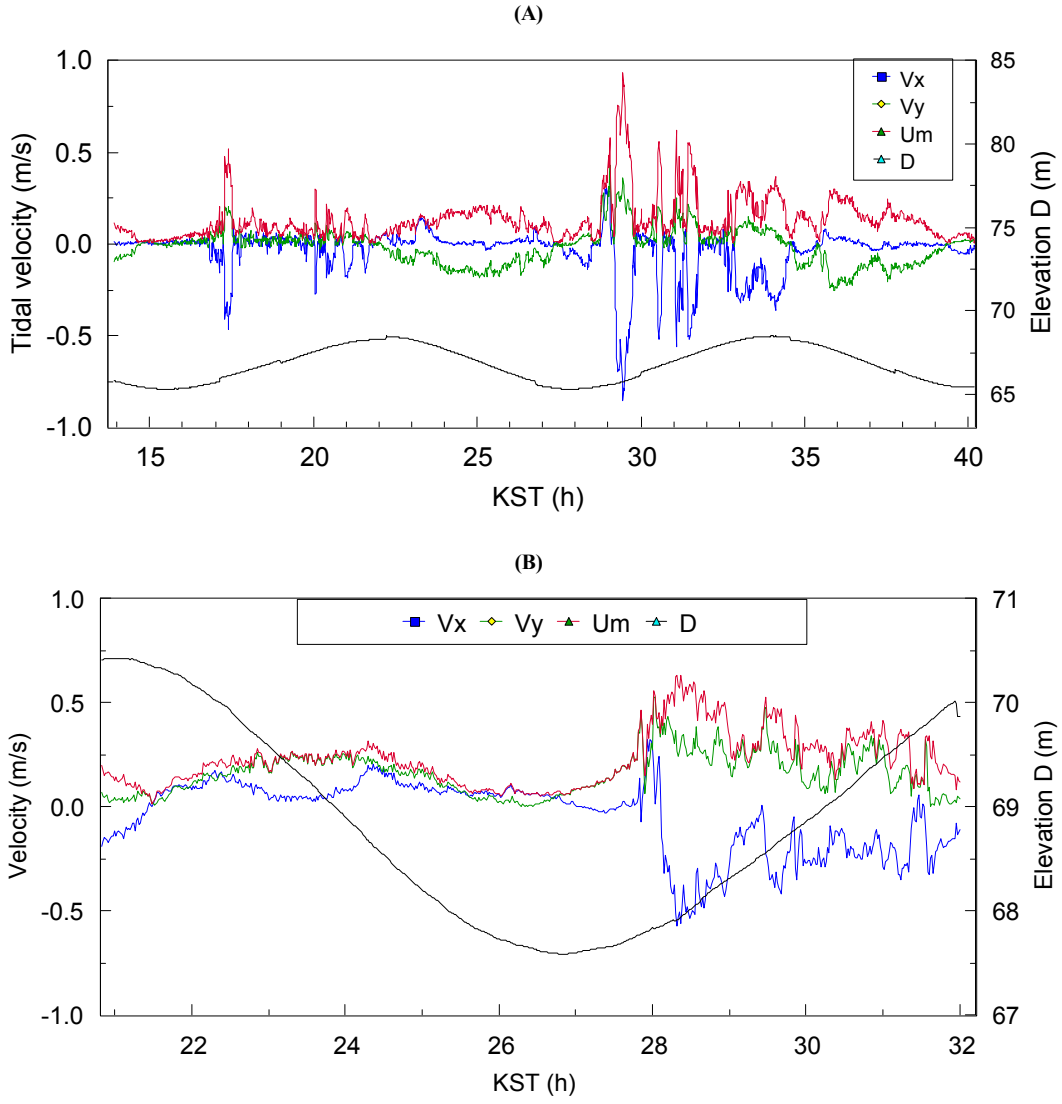

Fig. 5. Mean tidal flow indicated by easterly (V_x), northerly (V_y) and resultant velocity (U_m) sampled at 16 Hz for 1 min at Station S2 on 6 April 2012 (A), and at Station S6 on 30 March 2014 (B).

The intercept and slope along with correlation coefficients for Eqs. (4) and (5), respectively, are given in Table 3. Ek increased with increasing resultant velocity, while T_r decreased with increasing resultant velocity. Furthermore, the relationship between the resultant velocity and the kinetic energy and the resultant velocity and the turbulence intensity was significant (high correlation coefficient), with the exception of the turbulence intensity at S1, which exhibited a lower correlation coefficient. Thus, the main features of the velocity change in turbulence can be expressed accurately with the kinetic energy as absolute values in relation to the mean velocity rather than the relative values of turbulence intensity.

The turbulence kinetic energy at S3 was similar to the ~0.03 m^2/s^2 recorded in the eastern English Channel at 20 m above the seabed at 60-m water depth at a maximum flow velocity of 1 m/s (Korotenko and Senchev, 2011). In one study, the turbulence kinetic energy was adopted as the main cue in the reaction of blue crab at the post-larval stage in tank experiments (Saiz, 1994; Welch et al., 1999), while in another study, the turbulence kinetic energy was not considered in the effects of turbulence on the movements of swim

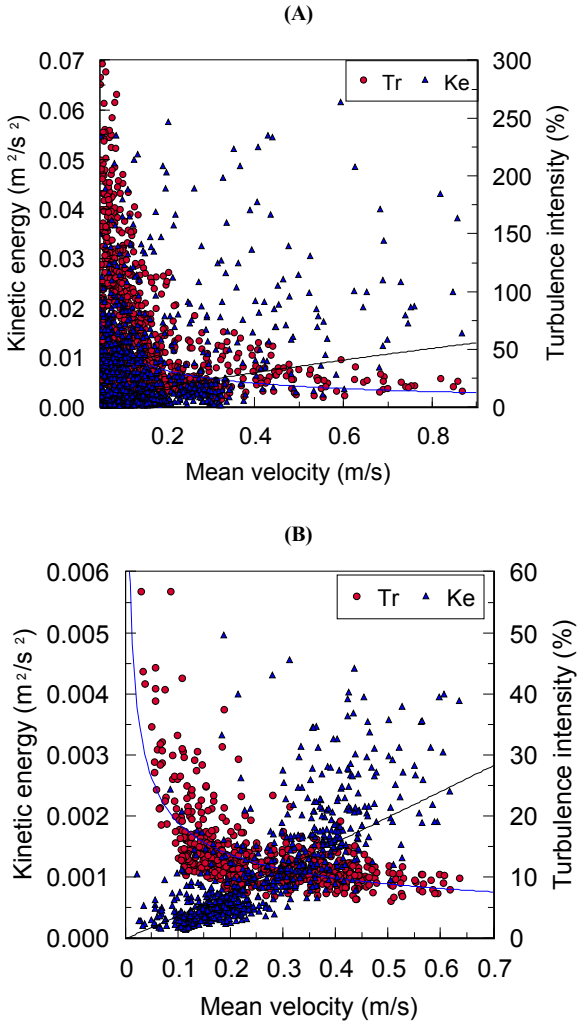

Fig. 6. Relationships between resultant mean velocity and turbulent kinetic energy (E_k) and turbulence intensity (T_r) at Stations S2 (A) and S3 (B).

ming salmon (Enders et al., 2003).

The FFT periodicity spectrum of the resultant velocity and flow direction for all sampling data from S2b are given in Fig. 7. Among the several peaks of period of <30 s, one dominant peak is observed around 10 s as a shorter period caused by oscillation of fishing gear or movements of fish. The shorter periods of velocity and direction produced by FFT ranged between 4 and 15 s, as shown in Table 4. Complex changes in tidal flow velocity with variations in flow direction have been observed to generally occur in near-bottom tidal flow (Roget et al., 2010; Walter et al., 2011). Because a shorter flow period could have greater effects on fish swimming or escape behavior (Kim et al., 2008), in this study we considered shorter only periods of ~10 s.

Table 3. The constants and slopes of the relationship between velocity (Vr) and kinetic energy (Ek) from Eq. (4) and Vr and the turbulence intensity (Tr) from Eq. (5)

Site	E_k			T_r			n*
	E_o	a	r	T_o	b	r	
S1	0.0016	1.62	0.80	7.47	-0.190	0.29	215
S2	0.0141	0.77	0.45	11.9	-0.615	0.62	1578
S3	0.0041	1.06	0.76	6.42	-0.472	0.72	638
S6	0.0053	1.19	0.65	7.68	-0.372	0.46	671

r: Correlation coefficient
*: Equal to sampling duration (min) in Table 2

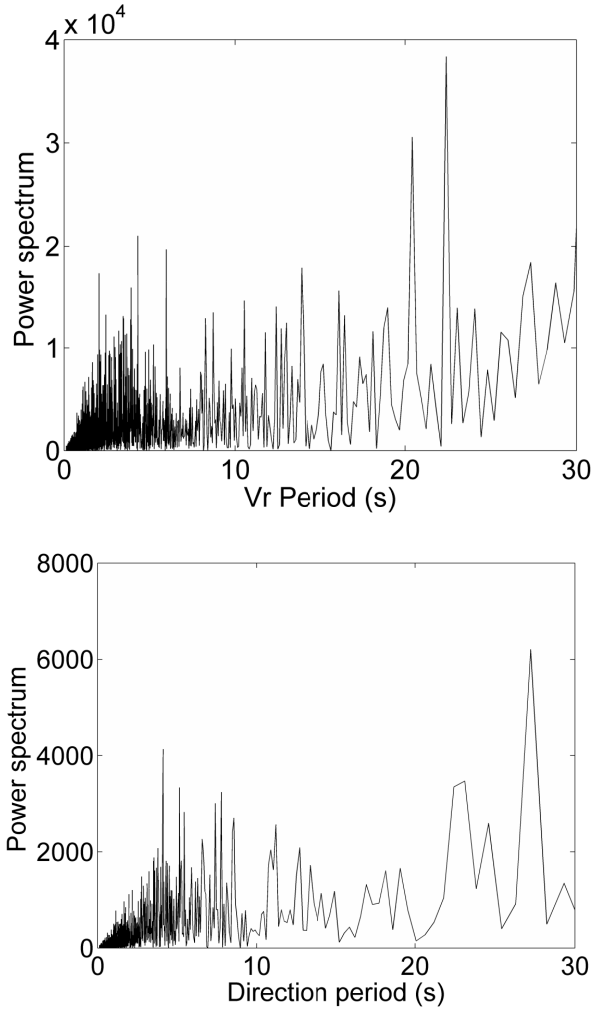

Fig. 7. Periodicity of resultant velocity Vr (A) and tidal direction (B) given by FFT of data recorded at 16 Hz at Station S2b on April 6 2012.

Fig. 8 shows the estimated period of velocity and direction using the global wavelet spectrum (GWL) method (Torrence

and Compo, 1998) for the eight scenarios of strong tide for periods <30 s given in Table 2. The dominant period of velocity and direction ranged between 4 and 17 s, while no peak period was present at S3a, S3b and S6a, as shown in Table 4.

The complex periodicity of tidal flow was examined using the continuous wavelet method with Morlet in MATLAB as shown in Fig. 9. The period plumes are clearly visible for shorter periods of 3–6 s, represented in blue, and the curves of the correlation coefficients are shown in the plots at the bottom of the figure. Although, we were unable to plot the entire analyzed period for each scenario, the shorter period of each flow velocity or direction appeared between 3 and 20 s, similar to the results yielded by the global wavelet method shown in Table 4. The periods produced by Morlet wavelet method for data recorded in Jiaozhou Bay, Qingdao, China at a water depth of 7 m and flow velocity of ~0.5 m/s with sampling at 16 Hz were estimated to be 4–64 s (Yuan et al., 2009). However, the periods produced by event detection method in the Eprapah Creek Estuary in eastern Australia at the seabed at a water depth of 2 m and flow velocity of ~0.25m/s with sampling at 50 Hz were estimated to be 0.25–1 s (Yuan et al., 2009). The results from these two studies are in agreement with the shorter periods of turbulent flow observed in our work. However, at a lower sampling rate of 2 Hz, the period at slack tide in Lunenburg Bay, Nova Scotia, Canada at a water depth of ~6 m and flow velocity of ~0.5 m/s ranged between 100 and 300 s (Rennie and Hay, 2008). This longer period was also observed in our study using the global wavelet and FFT methods.

Tables 5 and 6 show the mean period, and the amplitude of velocity and direction, respectively, produced by peak event analysis for the eight scenarios of strong tide in Table 2. The mean periods ranged between 4 and 8 s for velocity and direction with no significant difference between flood and ebb tides. The amplitude of the velocity variation ranged between 0.1 and 0.6 m/s and increased with increasing mean velocity. Similarly, the amplitude of the directional variation ranged between 20 and 90° and increased with increasing mean velocity. The period rate for peak or valley events ranged from at least 80 to 100% as covered time ratio of periodic events, while the pair rate of a consecutive pair of peak and valley events of period <30 s ranged between 30 and 70%. These rates are characteristic of the periodic ratios in highly variable data of turbulence flow similar to the coefficients yielded by the Morlet wavelet method. However, the peak event method can provide an estimate of the absolute range of amplitude for each period for comparison with other period analysis methods such as FFT or the wavelet method. The amplitude obtained by peak event analysis was considered as different terms in relation to the standard deviation, which was calculated for all data without periodic analysis (Bendat and Piersol, 2000).

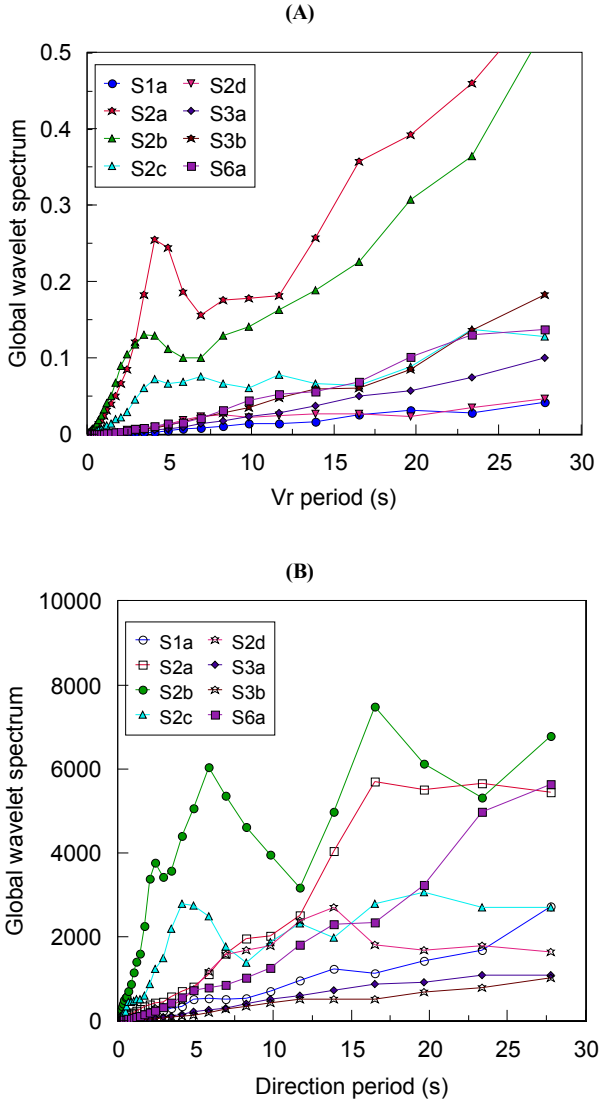

Fig. 8. Period of resultant velocity (A) and tidal direction (B) for eight scenarios of strong tide given in Table 2 estimated using global wavelet spectrum method.

Table 4. Peak period of tidal velocity and direction by FFT and the GWL method

Sample	Tide	Sample NO	Period by FFT (s)		Period by GWS (s)	
			Velocity	Direction	Velocity	Direction
S2a	Flood	16,820	4.9	6.4	4.1	16.5
S2b	Flood	25,800	4.3	6.1	3.5	2.5
S2c	Flood	12,200	4.1	5.0	4.1	4.1
S2d	Flood	15,600	6.0	5.4	8.3	13.9
S3b	Flood	45,000	13.4	8.9	na	13.9
S6a	Flood	36,100	10.7	14.8	na	na
S1a	Ebb	25,600	4.4	12.0	9.8	5.8
S3a	Ebb	80,400	10.5	7.9	na	na

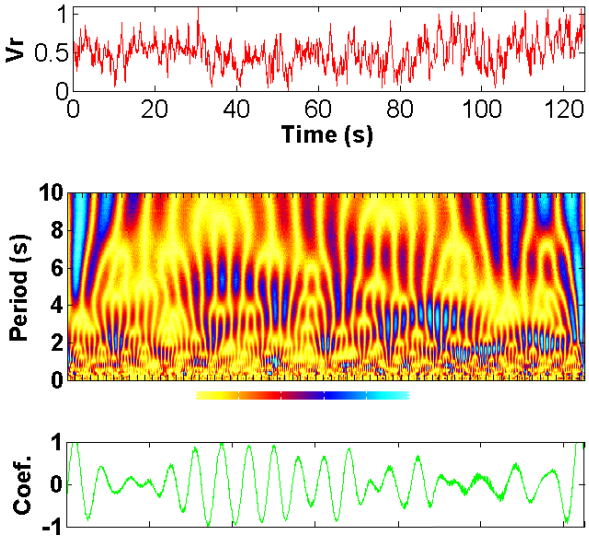

Fig. 9. Periodicities produced by continuous wavelet method with Morlet in MATLAB for resultant velocity Vr for 2000 sampling data (= 125s) at Station S2b. Colors from left to right represents higher periodic correlation, as shown in the plots at the middle of the figure.

The period frequencies of tidal velocity and tidal direction given by peak event analysis are shown in Fig. 10. When the minimum period was <1 s the peak periods ranged between 2 and 4 s for the tidal velocity, and between 1 and 3 s for the tidal direction.

The period of the swim speed variation of fish depends on body length and tail beat frequency and has been variously reported at between 0.1 and several seconds (Videler and Wardle, 1991). The dominant period of swimming acceleration in juvenile roundfish near the upper panel of the codend was 2~3 s at a towing speed of 1.5 m/s (Kim et al., 2008). The effect of turbulence on Atlantic salmon was investigated at a dominant flow period of 6 s in tank experiments. The dominant period of turbulence flow on the codend of the shrimp beam trawl or bottom trawl was estimated at between 3 and 8 s when a shorter period of <60 s was selected (Kim, 2012; 2013a) and its value is possibly related to the period of swimming response in escaped fish from the codend (Kim et al., 2008). Therefore, period analysis of shorter periods of a few seconds is suitable for studying the movements of swimming fish or fishing gear dynamics.

The turbulent water flow inside the codend could be resultant turbulence mixed up by tidal flow, towing motion of a fishing boat, wake of fishing gear, etc. In addition, the main index of turbulence effects on animal movements or swimming fish movements should be considered as kinetic energy, and the dominant period of tidal flow as 3-D and flow direction for analyzing the stability control of fish (Kim and Gordon, 2010; Webb and Cotel, 2010: Tritico and Cotel, 2010). Therefore, in future, turbulent mixing inside the codend should be analyzed and interpreted as complex flow including the tidal turbulence flow in the overlying water.

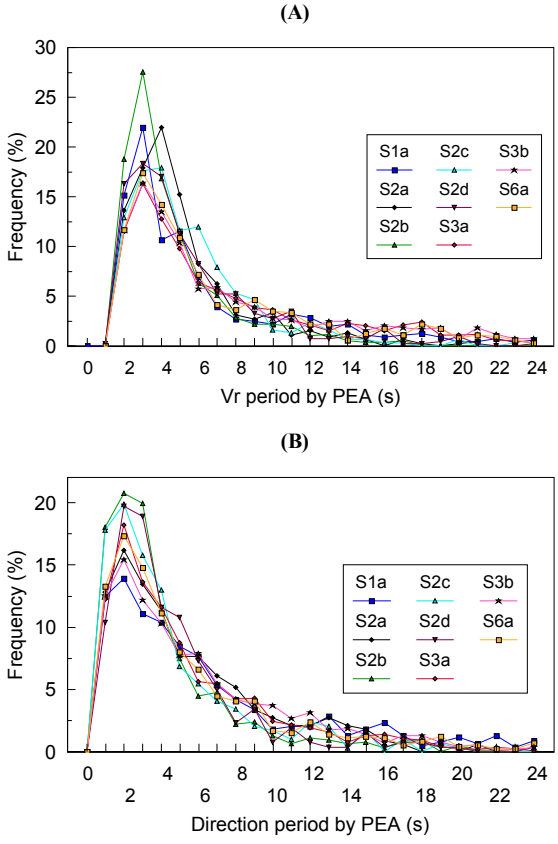

Fig. 10. Period frequencies of tidal velocity (A) and tidal direction (B) produced by peak event analysis.

Table 5. Velocity period and amplitude produced by peak event analysis

Sample	Tide	Duration (s)	Event* no.	Velocity (m/s)		Period (s)	Period rate** (%)	Pair no. & rate*** (%)
				mean±SD	range			
S2a	Flood	1,051	+229	0.72±0.14	0.52	4.6±3.1	99	147
			-217	0.17±0.11	0.55	4.8±3.4	100	65
S2b	Flood	1,613	+386	1.02±0.02	0.57	4.1±3.3	99	256
			-375	0.44±0.14	0.58	4.3±3.1	100	66
S2c	Flood	763	+157	0.65±0.10	0.35	4.8±3.2	99	104
			-144	0.30±0.09	0.35	5.3±3.5	100	69
S2d	Flood	975	+179	0.40±0.05	0.17	5.4±4.7	100	110
			-186	0.24±0.04	0.17	5.2±4.3	100	60
S3b	Flood	2,813	+382	0.60±0.07	0.17	7.1±6.0	96	190
			-380	0.42±0.06	0.18	7.4±6.1	100	49
S6a	Flood	2,256	+293	0.63±0.07	0.18	7.1±6.1	92	160
			-309	0.44±0.08	0.19	7.1±5.9	97	50
S1a	Ebb	3,200	+425	0.34±0.04	0.11	6.5±6.3	86	148
			-397	0.21±0.06	0.12	6.5±6.4	80	30
S3a	Ebb	5,025	+670	0.47±0.05	0.14	7.5±6.8	100	339
			- 672	0.33±0.04	0.14	7.5±6.5	100	50

* + : Peak, -: valley
** Mean period × event no. / duration
*** Mean period × pair no. / duration

Table 6. Tidal direction period and amplitude produced by peak event analysis

Sample	Tide	Duration (s)	Event* no.	Direction (°)		Period (s)	Period rate** (%)	Pair no. & rate*** (%)
				mean±SD	range			
S2a	Flood	1,051	+84	334±18	84	5.0±4.3	40	54
			-175	61±102	87	5.8±4.8	97	27
S2b	Flood	1,613	+315	315±13	59	4.4±3.5	85	218
			-312	238±84	77	5.1±4.2	99	64
S2c	Flood	763	+155	316±14	54	4.6±3.3	94	96
			-139	256±65	59	5.5±4.7	100	64
S2d	Flood	975	+167	297±6	33	5.8±4.5	100	104
			-162	262±33	35	6.0±4.1	99	63
S3b	Flood	2,813	+426	295±7	17	6.6±4.9	100	254
			-437	277±16	18	6.3±4.8	98	58
S6a	Flood	2,256	+360	315±12	18	6.0±5.1	95	198
			-351	293±24	22	6.2±5.1	97	54
S1a	Ebb	3,200	+366	80±19	18	7.4±6.1	84	176
			-410	59±21	21	7.0±6.0	89	39
S3a	Ebb	5,025	+857	77±6	19	5.8±4.5	99	483
			-808	57±7	20	6.2±4.8	100	58

*, **, *** Refer to Table 5

Acknowledgement

Authors thank captain K.M. Bae and crews of the Research ship Charmbada, and Skipper H.D. Moon of the fishing boat for assistance of field measurements and Prof. B.K. Choi and Dr. D.S. Gu for useful help in periodicity analysis. Wavelet software for global wavelet spectrum was available at : http://paos.colorado.edu/research/wavelet/ provided by C. Torrence and G. Compo. This work was supported by the Korea Research Foundation Grant funded by the Korean Government (NRF-2010-0022707).

References

Bendat JS and Piersol AG. 2000. Random data analysis and measurement procedures. 3rdEdition.John Wiley & Sons, Inc. Hoboken, New Jersey. p.349-456.

Bernard PS and Wallace JM. 2002. Turbulent flow. Analysis, measurement and prediction. John Wiley & Sons, Inc. Hoboken, New Jersey. 497p.

Bouhoubeiny E, Germain G and Druault P. 2011. Time-resolved PIV investigations of the flow field around cod-end net structures. Fish Res 108, 344-355.(doi:10.1016/j.fishres. 2011.01.010)

Chanson H. 2010. Unsteady turbulence in tidal bores: Effects of bed roughness. J Waterway, Coastal & Ocean Eng 136, 247-256.

Chanson H, Reungoat D, Simon B and Lubin P. 2011. High-frequency turbulence and suspended sediment concentration measurements in the Garonne River tidal bore. Estua Coast & Shelf Sci 95, 298-306.

Enders EC, Boisclair D and Roy AG. 2003. The effect of turbulence on the cost of swimming for juvenile Atlantic salmon (Salmo sala). Can J Aquat Sci 60, 1149-1160.(doi:10.1139/F03-101)

Ham R van der R, Fontijn HL, Kranenburg C and Winterwerp JC. 2001. Turbulent exchange of fine sediments in a tidal channel in the Ems/Dollard estuary. Part I : Turbulence measurements. Continen Shelf Res 21, 1605-1628.

Kim YH. 2012. Analysis of turbulence and tilt by in-situ measurements inside the codend of a shrimp beam trawl. Ocean Eng 53, 6-15. (http://dx.doi.org/10.1016/j.oceaneng.2012.06.014)

Kim YH. 2013a. Analysis of the turbulent flow and tilt by in the codend of a bottom trawl during fishing operation. Ocean Eng 64, 100-108. (http://dx.doi.org/10.1016/j.oceaneng.2013.02.019)

Kim YH. 2013b. Shaking motion characteristics of a cod-end caused by an attached circular canvas during tank experiments and sea trials. Fish Aquat Sci 16, 211-220.(http://dx.doi.org/ 10.5657/FAS.2013.0211)

Kim YH and Gordon MS. 2010. Swimming and posture control of common carp when penetrating mesh nets in water tunnel. Fish Res 102, 166-172.

Kim YH, Wardle CS and An YS. 2008. Herding and escaping responses of juvenile roundfish to square mesh window in a trawl cod end. Fish Sci 74, 1-7. (http://dx.doi.org/10.1111/j.1444-2906.2007.01490.x.)

Korotenko KA and Senchev AV. 2011. Turbulence investigation in a tidal coastal region. Oceanography 51, 394-406.

Liao JC. 2007. A review of fish swimming mechanics and behaviour in altered flows. Phil Trans R B 362, 1973-1993. (http://dx.doi.org/10.1098/rstb.2007.2082)

Liu H, Wu C and Wu J. 2009a. Contrast between estuarine and river systems in near-bed turbulent flows in the Zhujiang (Pearl River) Estuary, China. Estuar. Coast Shelf Sci 83, 591-601.

Liu Z, Wei H, Lozovatsky ID and Fernando HJS. 2009b. Late summer stratification, internal waves, and turbulence in the Yellow Sea. J Mar Syst 77, 459-472.

Lozovastsky I, Liu Z, Fernando H, Armengol J and Roget E. 2012. Shallow water tidal currents in close proximity to the seafloor and boundary-induced turbulence. Ocean Dyna 62, 177-191. (DOI:10.1007/s10236-011-0495-3)

Lupandin AI. 2005. Effect of flow turbulence on swimming speed of fish. Biol Bull 32, 461-466.

McLelland SJ and Nicholas AP. 2000. A new method for evaluating errors in high-frequency ADV measurements. Hydrol Proce 14, 351-365.

Narasimha R, Kumar SR, Prabhu A and Kailas SV. 2007. Turbulent flux events in a nearly neutral atmospheric boundary layer. Philos Trans R Soc A 365, 841-858. (http://dx.doi.org/ 10.1098/rsta.2006.1949)

O'Neill FG, McKay S, Ward JN, Strickland A, Kynoch RJ and Zuur AF. 2003. An investigation of the relationship between sea state induced vessel motion and cod-end selection. Fish Res 60, 107-130. (http://dx.doi.org/10.1016/S0165-7836(02)00056-5)

Parra SM, Marino-Tapia I, Enriquez C and Valle-Levinson A. 2014. Variations in turbulent kinetic energy at a point source submarine groundwater discharge in a reef lagoon. Ocean Dyna (doi:10.1007/s10236-014-0765-y)

Pichot G, Germain G and Priour D. 2009. On the experimental study of the flow around a fishing net. J Mech B/Fluids 28, 103-116. (http://dx.doi.org/10.1016/j.euromechflu.2008.02.002)

Rennie CD and Hay A. 2008. Reynolds stress estimates in a tidal channel from phase-wrapped ADV data. J Coastal Res 26, 157-166.

Rippeth TP, Simpson JH, Williams E and Inall ME. 2003. Measurements of the rates of production and dissipation of turbulent kinetic energy in an energetic tidal flow: Red Warf Bay revisited. J Phys Oceanogr 33, 1889-1901.

Roget E, Planella J, Fernando HJS and Liu Z. 2010. Intermittency

of near-bottom turbulence in tidal flow on a shallow shelf. Geophysical Res Oceans 115, C05006. 16p.

Saiz E. 1994. Observations of the free-swimming behaviour of *Acartia tonsa*: Effects of food concentration and turbulent water motion. Limnol Ocean 39, 1566-1578.

Seena A and Sung HJ. 2011. Wavelet spatial scaling for educing dynamic structures in turbulent open cavity flows. J Fluids Struct 27, 962-975.

Shadwick RE and Lauder GV. 2006. Fish biomehcnics. Fish physiology vol. 23. Academic Press. San Diego, USA. 542p.

Simpson JH, Williams E, Brasseur LH and Brubaker JM. 2005. The impact of tidal straining on the cycle of turbulence in a partially stratified estuary. Continen Shelf Res 25, 51-64.(doi:10.1016/j.csr.2004.08.003)

Thomson J, Polagye B, Durgesh V and Richmond MC. 2012. Measurements of turbulence at two tidal energy sites in Puget Sound, WA. IEEE J Oceanic Eng 37, 363-374.(DOI:10.1109/JOE.2012.2191656)

Thorpe SA. 2007. An introduction to ocean turbulence. Cambridge Univ. Press. UK. Ch. 1.(1-36) Ch.2(37-76) P. 267.

Thorpe SA, Green JAM and Simpson JH. 2008. Boils and turbulence in a weakly stratified shallow tidal sea. Am Meteorol Soc 38, 1711-1730.(DOI:10.1175/2008JPO3931.1)

Torrence C and Compo GP. 1998. A practical guide to wavelet analysis. Bull Am Meteorol Soc 79, 61-78.(http://dx.doi.org/10.1175/1520-0477(1998)079<0061:APGTWA>2.0.CO;2)

Tritico HM and Cotel AJ. 2010. The effects of turbulent eddies on the stability and critical swimming speed of creek chub (*Semotilus atromaculatus*). J Exp Biol 213, 2284-2293.(doi:10.1242/jeb.041806)

Videler JJ and Wardle CS. 1991. Fish swimming stride by stride: speed limits and endurance. Rev Fish Biol & Fish 1, 23-40.

Walter RK, Nidzieko NJ and Monismith SG. 2011. Similarity scaling of turbulence spectra and cospectra in a shallow tidal flow. J Geophysical Res Ocean 116, C10019. 14p.

Webb PW and Cotel AJ. 2010. Turbulence: Does vorticity affect the structure and shape of body and fin propulsors? Integ Comp Biol 50, 1155-1166.(http://dx.doi.org/10.1093/icb/icq020)

Welch JM, Forward jr RB and Howd PA. 1999. Behavioral responses of blue crab *Callinectes sapidus* postlarvae to turbulence: Implications for selective tidal stream transport. Mar Ecol Prog Ser 179, 135-143.

Yuan Y, Wei H, Zhao L and Cao Y. 2009. Implications of intermittent turbulent bursts for sediment resuspension in a coastal bottom boundary layer: A filed study in the western Yellow Sea, China. Mar Geol 263, 87-96.(doi:10.1016/j.margeo.2009.03.023)

Zhang Q, Xu CY and Chen YD. 2010. Wavelet-based characterization of water level behaviors in the Pearl river estuary, China Stoch Environ Res Risk Assess 24, 81-92.

2014.10.29 Received
2014.11.20 Revised
2014.11.21. Accepted